

# Tachyon stars

Ernst Trojan

*Moscow Institute of Physics and Technology*

*PO Box 3, Moscow, 125080, Russia*

June 6, 2021

## Abstract

We consider a self-gravitating body composed of ideal Fermi gas of tachyons at zero temperature. The Oppenheimer-Volkoff equation is solved for various central densities and various tachyon mass parameter  $m$ . Although a pure tachyon star has finite mass, it cannot occur in nature because the equilibrium condition  $P = 0$  and the causality condition cannot be satisfied simultaneously. A stable configuration with tachyon content must be covered with a non-tachyon envelope. The boundary between the tachyon core and the envelope is determined by the critical pressure  $P_T$ , which depends on the tachyon mass  $m$ . The tachyon core is dominant and its mass can exceed many times the solar mass  $M_\odot$  when  $m$  is much smaller than the nucleon mass  $m_p$ , while at large  $m$  compared with  $m_p$ , the main contribution to the total stellar mass is due to the envelope whose material determines the parameters of the whole star. However, the parameters of the tachyon core do not depend on the envelope material. When the tachyon core appears, its mass  $M_T$  and radius  $r_T$  grow up with increasing central density until maximum values are reached, after which the mass and radius slowly decrease. The redshift at the surface of the tachyon core does not depend on  $m$  and never exceeds  $z_{\max} \simeq 0.3$ . The maximum mass of tachyon core and its maximum radius are achieved at certain central density and obey universal formulas  $M_{T\max}/M_\odot = 0.52m_p^2/m^2$  and  $r_{T\max}[\text{km}] = 4.07m_p^2/m^2$  that allow to estimate arbitrary supermassive tachyonic bodies at the cosmological scale.

# 1 Introduction

Tachyons are instabilities of the field theory with the energy spectrum:

$$\varepsilon_k = \sqrt{k^2 - m^2} \quad (1)$$

where  $m$  is the tachyon mass. Tachyons are usually considered in cosmological models [1, 2, 3, 4, 5], and a system of many tachyons is studied in the frames of statistical mechanics [6, 7, 8]. An ensemble of many tachyons can be considered as a stable continuous medium when it satisfies the causality

$$c_s^2 = \frac{dP}{dE} \leq 1 \quad (2)$$

that implies that the sound speed  $c_s$  is subluminal, and that the functional dependence  $P[E]$  between the pressure  $P$  and energy density  $E$ , called as the equation of state (EOS), reveals 'good' behavior. Otherwise, the system will not be stable with respect to sound perturbations. It implies that no stable tachyon matter can have free surface with  $P = 0$ . Thus, if we consider a static self-gravitating macroscopic tachyon body, it must be embedded in a non-tachyon envelope. Since the tachyon matter is often discussed in cosmological problems, and it is important to know whether macroscopic tachyonic objects can exist and what is their maximum mass. If the mass of the body is great enough, its gravitational collapse cannot be counterbalanced by the pressure, and it is necessary to establish the upper bound for the mass until the body becomes a black hole.

In the present paper we consider a tachyon Fermi gas at zero temperature which satisfies the causality (2) when its energy density and pressure exceed critical values [9]

$$E_T = \frac{\gamma m^4}{16\pi^2} \left[ \sqrt{3} - \ln \left( \sqrt{\frac{3}{2}} + \frac{1}{\sqrt{2}} \right) \right] \quad (3)$$

$$P_T = \frac{\gamma m^4}{16\pi^2} \left[ \sqrt{3} + \ln \left( \sqrt{\frac{3}{2}} + \frac{1}{\sqrt{2}} \right) \right] \quad (4)$$

corresponding to the critical Fermi momentum

$$k_T = \sqrt{\frac{3}{2}} m \quad (5)$$

where  $\gamma = 1$  is the tachyon degeneracy factor. The tachyon pressure never turns to zero, and tachyon matter cannot have free surface, it must be dressed in non-tachyon envelope. The tachyon matter is endowed with another peculiar property: its pressure decreases when its energy density grows up (see Fig. 1), and ultra-relativistic EOS

$$P = \frac{E}{3} \quad (6)$$

is achieved at large energy density (when  $k_F \gg m$ ), while the tachyon EOS becomes 'absolute stiff'

$$P = E \quad (7)$$

and even 'hyperstiff'

$$P > E \quad (8)$$

at low density when  $k_F \rightarrow k_T$  (particularly,  $P_T = 2.23E_T$ ). So, a compact cosmic object with tachyon content may be endowed with strange properties. We consider the simplest example of a static spherical self-gravitating body with tachyon core and non-tachyon envelope, calculate its parameters and find the maximum mass of the tachyon core.

Standard relativistic units  $c_{light} = \hbar = G = 1$  are used in the article.

## 2 Tachyon Fermi gas

The thermodynamical functions of a system of free particles with the tachyonic energy spectrum  $\varepsilon_k$  (1) are determined by standard formulas of statistical mechanics. Particularly, the energy density and pressure of a tachyon Fermi gas at zero temperature are [9]:

$$E = \frac{\gamma m^4}{8\pi^2} \left[ \beta^3 \sqrt{\beta^2 - 1} - \frac{1}{2} \beta \sqrt{\beta^2 - 1} - \frac{1}{2} \ln \left( \beta + \sqrt{\beta^2 - 1} \right) \right] \quad (9)$$

and

$$P = \frac{\gamma m^4}{8\pi^2} \left[ \frac{1}{3} \beta^3 \sqrt{\beta^2 - 1} + \frac{1}{2} \beta \sqrt{\beta^2 - 1} + \frac{1}{2} \ln \left( \beta + \sqrt{\beta^2 - 1} \right) \right] \quad (10)$$

where dimensionless variable

$$\beta = \frac{k_F}{m} \quad (11)$$

depends on the Fermi-momentum  $k_F$  which is linked with the particle number density according to standard expression [13]

$$n = \frac{\gamma k_F^3}{6\pi^2} \quad (12)$$

so that the density is given in the form

$$\rho = mn = \frac{\gamma m k_F^3}{6\pi^2} = \frac{\gamma m^4}{6\pi^2} \beta^3 \quad (13)$$

It is convenient to express all parameters of tachyon matter in the unit of normal nuclear density

$$\rho_0 = m_p n_0 = 2.7 \times 10^{14} \text{ g} \cdot \text{cm}^{-3} = 157 \text{ MeV} \cdot \text{fm}^{-3} \quad (14)$$

where  $m_p$  is the nucleon mass and

$$n_0 = \frac{4 (1.36 \text{ fm}^{-1})^3}{6\pi^2} \cong 0.17 \text{ fm}^{-3} \quad (15)$$

is the saturation particle number density of symmetric nuclear matter [12]. Thus, dividing (9), (10) and (13) by (14), we have

$$\frac{E}{\rho_0} = \frac{\gamma m^3}{8\pi^2 n_0 m_p} \left[ \beta^3 \sqrt{\beta^2 - 1} - \frac{1}{2} \beta \sqrt{\beta^2 - 1} - \frac{1}{2} \ln \left( \beta + \sqrt{\beta^2 - 1} \right) \right] \quad (16)$$

$$\frac{P}{\rho_0} = \frac{\gamma m^3}{8\pi^2 n_0 m_p} \left[ \frac{1}{3} \beta^3 \sqrt{\beta^2 - 1} + \frac{1}{2} \beta \sqrt{\beta^2 - 1} + \frac{1}{2} \ln \left( \beta + \sqrt{\beta^2 - 1} \right) \right] \quad (17)$$

$$\frac{\rho}{\rho_0} = \frac{mn}{m_p n_0} = \frac{\gamma k_F^3}{6\pi^2 n_0} \frac{m}{m_p} = \frac{\gamma m^3}{6\pi^2 n_0 m_p} \beta^3 \quad (18)$$

Momentum  $k = 1 \text{ fm}^{-1}$  corresponds to energy  $\varepsilon_k = k = 198 \text{ MeV}$ :

$$1 \text{ fm}^{-1} \leftrightarrow 198 \text{ MeV} \quad (19)$$

while  $k = 4.74 \text{ fm}^{-1}$  corresponds to the mass of nucleon  $m_p = 939 \text{ MeV}$ , and normal nuclear density (14) corresponds to

$$\rho_0 \leftrightarrow 0.80 \text{ fm}^{-4} \quad (20)$$

The tachyon mass parameter  $m$  plays the role of form-factor in equations (16)-(18). Taking  $m = 4.74\bar{m} = 4.74m/m_p$ , we find that

$$\frac{m^3}{2\pi^2 n_0} \frac{m}{m_p} = \frac{(4.74)^3}{2\pi^2 \cdot 0.17} \frac{m^4}{m_p^4} = 31.74\bar{m}^4 \quad (21)$$

Hence, substituting (21) in (16)-(18), we express the energy density and pressure in nuclear units:

$$\frac{E}{\rho_0} = 7.93\gamma\bar{m}^4 \left[ \beta^3 \sqrt{\beta^2 - 1} - \frac{1}{2}\beta \sqrt{\beta^2 - 1} - \frac{1}{2} \ln \left( \beta + \sqrt{\beta^2 - 1} \right) \right] \equiv \bar{E}\bar{m}^4 \quad (22)$$

$$\frac{P}{\rho_0} = 7.93\gamma\bar{m}^4 \left[ \frac{1}{3}\beta^3 \sqrt{\beta^2 - 1} + \frac{1}{2}\beta \sqrt{\beta^2 - 1} + \frac{1}{2} \ln \left( \beta + \sqrt{\beta^2 - 1} \right) \right] \equiv \bar{P}\bar{m}^4 \quad (23)$$

$$\frac{\rho}{\rho_0} = 10.58\gamma\bar{m}^4 \beta^3 \equiv \bar{\rho}\bar{m}^4 \quad (24)$$

where dimensionless  $\bar{E}$ ,  $\bar{P}$  and  $\bar{\rho}$  imply the energy density, pressure and density of tachyon gas with  $m = m_p$ .

By the way, the well-known EOS of the ordinary Fermi gas of subluminal particles with the energy spectrum

$$\varepsilon_k = \sqrt{k^2 + m^2} \quad (25)$$

can be given in the universal form

$$E = \frac{\gamma m^4}{8\pi^2} \left[ \beta^3 \sqrt{\beta^2 + 1} - \frac{1}{2}\beta \sqrt{\beta^2 + 1} - \frac{1}{2} \ln \left( \beta + \sqrt{\beta^2 + 1} \right) \right] \quad (26)$$

$$P = \frac{\gamma m^4}{8\pi^2} \left[ \frac{1}{3}\beta^3 \sqrt{\beta^2 + 1} + \frac{1}{2}\beta \sqrt{\beta^2 + 1} + \frac{1}{2} \ln \left( \beta + \sqrt{\beta^2 + 1} \right) \right] \quad (27)$$

that also includes dimensionless variable  $\beta$  (11) and the same form-factor  $\bar{m}^4$ . Both tachyon and bradyon EOS tend to the same ultra-relativistic limit

$$P = \frac{E}{3} \simeq \frac{\gamma m^4}{24\pi^2} \beta^4 \sim n^{4/3} \quad (28)$$

when  $\beta \rightarrow \infty$ . However the tachyon EOS reveals the following non-relativistic ( $\beta \rightarrow 1$ ) behavior

$$P \rightarrow \frac{\gamma\sqrt{2}m^4}{4\pi^2} \sqrt{\beta-1} = \frac{\gamma m^4}{4\pi^2} \sqrt{\frac{2}{3} \left( \frac{n}{n_0} - 1 \right)} \gg E \rightarrow \frac{\gamma\sqrt{2}m^4}{3\pi^2} (\sqrt{\beta-1})^3 = \frac{\gamma m^4}{3\pi^2} \sqrt{\frac{2}{3} \left( \frac{n}{n_0} - 1 \right)}^3 \quad (29)$$

while the EOS of non-relativistic ( $\beta \rightarrow 0$ ) bradyons obeys standard formulas

$$P \rightarrow \frac{\gamma m^4 \beta^5}{30\pi^2} = \frac{(6\pi^2/\gamma)^{2/3}}{5m} n^{5/3} \quad E \rightarrow mn + \frac{3}{2}P \quad n \rightarrow 0 \sqrt{\frac{2}{3} \left( \frac{6\pi^2 n}{\gamma} - 1 \right)} \quad n = 1 + \frac{1}{3} \frac{x}{n_0} \quad (30)$$

Dependence of ratio  $P/E$  vs  $\beta$  is given in Fig. 1. The EOS of cold tachyon Fermi (22)-(23) is hyperstiff (8) when [9]

$$\beta < \beta_1 = 1.529 \quad (31)$$

However, the variable  $\beta$  cannot be arbitrary small because the tachyonic parameters (9)-(10) satisfy the causality condition (2) when the Fermi momentum exceeds the critical value (5) corresponding to

$$\beta \geq \beta_T = \sqrt{\frac{3}{2}} \cong 1.225 \quad (32)$$

and no stable tachyon matter exists at low density

$$\rho < \rho_T = \frac{\gamma m^4}{6\pi^2} \left( \frac{3}{2} \right)^{3/2} \quad (33)$$

while the energy density and pressure cannot fall below critical minimum values (3) and (4). The critical parameters (33), (3) and (4) are

$$\frac{E_T}{\rho_0} = 4.26\gamma\bar{m}^4 \quad (34)$$

$$\frac{P_T}{\rho_0} = 9.48\gamma\bar{m}^4 \quad (35)$$

$$\frac{\rho_T}{\rho_0} = 19.44\gamma\bar{m}^4 \quad (36)$$

The critical density (36) differs from the value  $\rho_T$  obtained in the previous research [9] where the tachyon particle number density was defined as

$$n = \frac{\gamma}{6\pi^2} (k_F^3 - m^3) \quad (37)$$

that is not correct [13]. Now we use the correct definition (12) that yields zero entropy of the cold tachyon Fermi gas in agreement with the Nernst heat theorem because  $E + P - \varepsilon_F n = 0$ , according to (9), (10) and (13), where  $\varepsilon_F = \sqrt{k_F^2 - m^2}$  is the Fermi energy of tachyon gas.

### 3 Properties of pure tachyon star

A stable spherical-symmetric configuration of self-gravitating body is determined by the Oppenheimer-Volkoff equation [14]:

$$\frac{dP}{dr} = -(E + P) \frac{M + 4\pi r^3 P}{r(r - 2M)} \quad (38)$$

where

$$\frac{dM}{dr} = 4\pi r^2 E \quad (39)$$

and  $M(r)$  is the mass distribution along radius  $r$ . Equations (38)-(39) must be solved under the initial conditions  $M(0) = 0$  and  $E_* = E(0)$ . The latter can be formulated in the form  $P_* = P(0)$  or  $\rho_* = \rho(0)$ . The boundary condition

$$P(r_*) = 0 \quad (40)$$

determines the total mass of the body  $M_* = M(r_*)$  and its radius  $r_*$ . Therefore, parameters,  $M_*$  and  $r_*$  depend on the EOS and the central density  $\rho_*$ .

Equations (38)-(39) allow to determine the upper bound of the mass until the body becomes a black hole. In general, the stiffer the EOS, the greater the mass of the star. The Oppenheimer-Volkoff limit  $M_* = 0.71M_\odot$  is obtained with non-interacting neutron gas. This limit becomes much greater for interacting neutron-rich matter, particularly,  $M_* = 1.64M_\odot$  for the EOS calculated in the frames of nonlinear sigma-model [10]. The maximum possible stellar mass  $M_* = 2.9 \div 3.2M_\odot$  [15, 16] is obtained when the 'absolute stiff' EOS (7) is applied.

However, a self-gravitating body composed of the tachyon matter may reveal unexpected 'hyperstiff' behavior (8), see Fig. 1. The tachyon matter in the dense center of the star will be 'soft', and its 'stiffness' will increase from the center to the edges where the density is smaller. Contrary to the gas of subluminal massive particles, the tachyon matter at low density (when  $\beta = k_F/m \rightarrow 1$ ) cannot be described by simple polytrope (28)-(29). It implies that a tachyon compact stellar object may have much more greater mass than the stars composed of regular matter and even 'absolute stiff' matter.

Substituting (22) and (23) in (38)-(39), we write equations in the dimensionless form

$$\frac{d\bar{P}}{dr} = -0.148(\bar{E} + \bar{P}) \frac{M + 1.77\bar{m}^4 r^3 \bar{P}}{r(r - 0.295M)} \quad (41)$$

$$\frac{dM}{dr} = 1.77\bar{m}^4 r^2 \bar{E} \quad (42)$$

where  $M$  is expressed in the unit of solar mass  $M_\odot = 1.99 \times 10^{33}$  g, and  $r$  is expressed in 10 km. Here the dimensionless form-factor  $\bar{m} = m/m_p$  plays the role of scaling. Substituting

$$\bar{M} = M\bar{m}^2 \quad \bar{r} = r\bar{m}^2 \quad (43)$$

in (41)-(42) we rewrite the equations so

$$\frac{d\bar{P}}{d\bar{r}} = -0.148(\bar{E} + \bar{P}) \frac{\bar{M} + 1.77\bar{r}^3 \bar{P}}{\bar{r}(\bar{r} - 0.295\bar{M})} \quad (44)$$

$$\frac{d\bar{M}}{d\bar{r}} = 1.77\bar{r}^2 \bar{E} \quad (45)$$

where  $\bar{M}$  is expressed in the unit of  $M_\odot \bar{m}^2$ , and  $\bar{r}$  is expressed in  $10\bar{m}^2$  km.

So, we need to simulate equations (44)-(45) in order to find the total mass  $\bar{M}_*$  and radius  $\bar{r}_*$ , while the stellar parameters at arbitrary  $m = \bar{m}m_p$  will be automatically determined, according to scaling (43), so

$$M_* = \frac{\bar{M}_*}{\bar{m}^2} \quad r_* = \frac{\bar{r}_*}{\bar{m}^2} \quad (46)$$

The theory states that the maximal mass of neutron stars is achieved when the central density  $\rho_* = 5 \div 10\rho_0$  [10, 16], depending on the particular model of nuclear matter. The relevant central density in a tachyon



self-gravitating body may vary in much more wider range, depending on the choice of the tachyon mass  $m$ . So, it is convenient to operate with dimensionless Fermi momentum  $\beta$  (11) rather than tachyon density  $\rho = 10.58\rho_0\bar{m}^4\beta^3$  (24). Now we need to find only one profile  $\bar{M}_*$  vs  $\beta_*$  in order to build all other profiles at different  $m$ , applying rescaling of the mass  $M_*$  (46).

The similar scaling (43) is applied to the Oppenheimer-Volkoff equation when operate with the EOS of cold Fermi gas of subluminal particles [14]. Of course, we can immediately calculate an ordinary neutron star with pure neutron content, substituting the EOS of subluminal Fermi gas (26)-(27) in (44)-(45). This star will always have finite mass and finite radius because the pressure turns to zero at finite  $\bar{r}_*$  (which depends on the central parameter  $\beta_*$  and form-factor  $m$ ). Indeed, it is due to the behavior of tachyonic thermodynamical functions (29)-(30) at  $\beta \rightarrow 1$  (see Fig. 1).

Results of calculation for a pure tachyon body are given in Fig. 2-6. The stellar mass  $\bar{M}_*$  is finite (Fig. 2), while its radius tends to infinity because the hydrostatic equilibrium  $\bar{P}(\bar{r}_*) = 0$  is achieved when  $\bar{r}_* \rightarrow \infty$ . In fact the tachyonic pressure never turns to zero.

So, we can estimate an effective radius  $\bar{r}_{90}$  together with  $\bar{r}_{99}$  under which only 90% and 99% of the total mass is enclosed, respectively (dashed and dotted vertical lines in Fig. 2). The effective radius of tachyon star remains almost constant

$$\bar{r}_* \equiv \bar{r}_{99} \simeq 50 \text{ km} \quad (47)$$

when the dimensionless Fermi momentum is large  $\beta_* > 2$  (Fig. 5), and  $\bar{r}_{99}$  increases, tending to infinity, when  $\beta_* \rightarrow 1$ .

The maximum mass of tachyon star

$$\bar{M}_{*\text{max}} = 1.18M_\odot \quad (48)$$

is achieved at

$$\beta_* = 1.81 \quad (49)$$

corresponding to the central density

$$\rho_* = 62.7\rho_0 \quad (50)$$

see Fig. 3 and Fig. 4).

Relation (43) implies that the redshift

$$z = \frac{1}{\sqrt{1 - 2M/r}} - 1 = \frac{1}{\sqrt{1 - 0.295\bar{M}/\bar{r}}} - 1 \quad (51)$$

does not depend on the tachyon mass  $m$ . The redshift attains its maximum  $z_{\max}$  inside the star and decreases closer to the surface (Fig. 6). The value  $z_{\max}$  increases with increase of the central parameter  $\beta_*$ , tending to  $z_{\max} \simeq 0.41$  at  $\beta_* \rightarrow \infty$ . Substituting the effective radius (47) in (51), we can define the effective surface redshift

$$z_{99} = 0.036 \quad (52)$$

associated with  $\bar{r}_{99}$  (47) that remains the same without regard of  $m$ .

We have determined the parameters of tachyon star at  $\bar{m} = m/m_p = 1$ , and, according to rescaling (46) we can immediately calculate the stellar parameters at arbitrary  $m$ , namely the maximum mass

$$M_{*\max} = \frac{1.18M_\odot}{\bar{m}^2} \quad (53)$$

is achieved at the central density

$$\rho_{*\max} = 62.7\rho_0\bar{m}^4 \quad (54)$$

corresponding to the same  $\beta_{*\max} = 1.81$  (49), while the effective radius of the star is

$$r_* \equiv r_{99} = \frac{50 \text{ km}}{\bar{m}^2} \quad (55)$$

For example, at  $m = 266 \text{ MeV}$  the maximum mass of tachyon star is

$$M_* = 14.7M_\odot \quad (56)$$

and its effective radius is

$$r_* \equiv r_{99} = 623 \text{ km} \quad (57)$$

The maximal mass (56) is achieved at the central density  $\rho_* = 0.41\rho_0$ .

According to equations (44)-(45), we have calculate self-gravitating body composed of pure tachyon matter, whose density is considered to be arbitrary low at the surface, when  $P \rightarrow 0$  at  $r \rightarrow \infty$ . Meanwhile the tachyon matter does not satisfy the causality (2) when  $\beta_F < \beta_T = \sqrt{3/2}$  (5) and  $P < P_T$  (4). It implies that no stable stellar configuration of pure tachyon matter is possible in practice. So, we need to revise the results in the light of realistic model which could have practical significance.

## 4 Tachyon core in non-tachyonic envelope

The stable tachyon matter cannot have free surface with  $P = 0$  because it cannot satisfy the causality (2) at arbitrary small density  $\rho$ , smaller than  $\rho_T$  (33), and its pressure cannot fall below the critical value  $P_T$  (4). Therefore, if the tachyon matter appears in some macroscopic domain, it must be dressed in a non-tachyonic envelope where hydrostatic equilibrium (40) could be achieved. Hence, the radius of such stellar configuration  $r_*$  will be greater than the radius of tachyon core  $r_T$  determined from condition  $P(r_T) = P_T$ . The mass of tachyon core  $M_T = M(r_T)$  will be smaller than the total mass of the body  $M_* = M(r_*)$  where  $r_*$  is found from condition  $P(r_*) = 0$  (40).

Let us analyze a stable configuration of tachyonic self-gravitating body immersed in some non-tachyonic medium. The tachyon core exists in the central region where the pressures exceeds the critical value  $P > P_T$  (35), corresponding to density  $\rho > \rho_T$  (36) and Fermi momentum  $k > k_T$  (5). The non-tachyonic envelope exists at  $P < P_T$ , and the boundary between the tachyon core and the envelope is determined as

$$P_T = P_{env} \quad (58)$$

where the pressure  $P_{env}$  is calculated with the particular EOS of the envelope. (It should be noted that the upper density in the envelope  $\rho_{env}$ , in general, does not coincide with  $\rho_T$ ).

We consider three variants of non-tachyonic material. The simplest idea is to put the tachyon core into a pure neutron (PN) envelope whose EOS is given by formulas (22)-(23) at  $m = m_p$ . For the envelope composed of 'absolute stiff' (AS) neutron matter its EOS  $P = E$  (7) is applied when  $\rho > \rho_s = 4.6 \times 10^{14} \text{ g} \cdot \text{cm}^{-3}$  and the Baym-Pethick-Sutherland (BPS) EOS [17] is applied when  $\rho < \rho_s$  [15]. Both PN and AS EOS are no more than limiting theoretical possibilities, while the real nuclear matter includes strong interaction and its EOS is stiffer than PN EOS but softer than AS EOS. For a reliable example we consider the neutron-rich matter in the nonlinear sigma model (NSM) [10, 11]. This NSM EOS was calculated at a high accuracy, including the effect of correlation energy, and its EOS stands between PN and AS – by these three alternatives we manage to embrace the whole range of possible envelope materials. The BPS EOS is applied when the density in the envelope becomes smaller than  $\rho_{\perp} = 2.5 \times 10^{14} \text{ g} \cdot \text{cm}^{-3}$  (although the outer layers at so small density do not affect the result).

The mass and radius of this stellar configuration is always finite, and it may depend on the sort of the envelope. At  $\beta_* < \sqrt{3/2}$  the star has no tachyon content and we do not discuss this range of densities in detail because the parameters of ordinary non-tachyonic neutron stars are already calculated [10, 14, 15, 16]. We calculate the total mass  $M_*$  and radius  $r_*$  as well as the mass of tachyon core  $M_T$  and its radius  $r_T$  at different dimensionless Fermi momentum  $\beta_* \geq \sqrt{3/2}$  (corresponding to the central density  $\rho_* \geq \rho_T$ ) and for several values of  $m$ , see Fig. 7-14.

When the tachyon mass equals to the nucleon mass  $m = m_p = 939$  MeV and the tachyon critical density is  $\rho_T = 19.44\rho_0$ , the total mass of the star is around  $M_* \simeq 1.3M_\odot$ ,  $M_* \simeq 1.4M_\odot$  and  $M_* \simeq 2.9M_\odot$  for the star with PN, NSM and AS envelope, respectively, while its total radius is around 6 km, 9 km, and 16 km and , see Fig. 7 and Fig. 8. While the total stellar mass is definitely greater than the relevant mass of non-tachyon star, the total radius is subject to no visible growth (the negligible increment round 0.5 km is not depicted in Fig. 8). The envelope makes major contribution to the total stellar mass, and the sort of material is very important here. The PN envelope is most sensible and its mass has increased almost three times with respect to the mass of PN star without the tachyon content.

As for the parameters of the tachyon core, they do not depend on the envelope material. The tachyon core appears in the star as soon as  $\beta_*$  exceeds  $\sqrt{3/2}$  and its mass and radius increase with increasing  $\beta_*$  until maximum values  $M_T = 0.52M_\odot$  and  $r_T = 4.07$  km are reached, after which the mass and radius decrease, see Fig. 7. The radius of tachyon core remains finite and it is almost a constant around 3.5 km at large  $\beta_*$  (Fig. 8).

Since the parameters of the tachyon core do not depend on the envelope EOS, we may choose the simplest variant of PN envelope to investigate the system at different tachyon mass  $m$ . At  $m = 666$  MeV ( $\rho_T = 4.91\rho_0$ ) the maximum mass of tachyon core is  $M_T = 1.02M_\odot$  and its maximum radius is  $r_T = 8.1$  km, while the mass of the whole stellar mass is around  $M_* = 2.4M_\odot$ , and its radius does not exceed 10 km (see Fig. 9). At  $m = 400$  MeV ( $\rho_T = 0.64\rho_0$ ) the maximum mass of tachyon core is  $M_T = 2.85M_\odot$  and its maximum radius approaches 22.4 km, while the total stellar mass is around  $M_* = 6.0M_\odot$ , and its radius does not exceed 25 km, (see Fig. 10). At  $m = 233$  MeV ( $\rho_T = 0.07\rho_0$ ) the tachyon core dominates over the envelope, without regard of its material (see Fig. 11). The maximum mass of tachyon core is  $M_T = 8.28M_\odot$  and its maximum radius is expanded up to  $r_T = 66$  km. However, the total stellar mass is around  $M_* = 9.0M_\odot$ , and its radius never

exceeds  $r_* = 70$  km. Now the tachyon core plays much more important role and its appearance is reflected in visible changes of the total stellar parameters, while the contribution of the envelope is small. At  $m = m_p = 138$  MeV the mass of tachyon core becomes as large as  $M_T = 23.7M_\odot$  and its maximum radius is around 188 km (see Fig. 12), while the envelope is thin and light and its contribution is negligible so that  $M_* \simeq M_T$  and  $r_* \simeq r_T$ .

However, the only calculation 13 is enough because, without regard of the envelope EOS, all profiles of the tachyon core obey the same scaling

$$M_T [\beta_*] = \frac{\bar{M}_T [\beta_*]}{\bar{m}^2} \quad r_T [\beta_*] = \frac{\bar{r}_T [\beta_*]}{\bar{m}^2} \quad (59)$$

where profiles  $\bar{M}_T [\beta_*]$  and  $\bar{r}_T [\beta_*]$  (see Fig. 13) are calculated at  $\bar{m} = m/m_p = 1$ . It should be also noted that the maximum mass  $M_{T \max}$  is achieved at the same  $\beta_{\max} = 2.18$ , while the maximum radius  $r_{T \max}$  is achieved at the same  $\beta_* = 1.61$ .

The scaling (59) implies that the redshift at the surface of the tachyon core is the same for every  $m$  (see Fig. 14) while the maximum value  $z_{T \max} = 0.30$  is achieved at the same  $\beta_* = 2.59$  without regard of  $m$ .

## 5 Conclusion

The thermodynamical functions of the cold tachyon Fermi gas (22)-(23) include the same form-factor  $\sim m^4$  as the EOS of cold Fermi gas of subluminal particles (26)-(27), but the tachyonic EOS may occur 'hyperstiff'  $P > E$  (see Fig. 1), and it makes sufficient difference from the usual analysis of neutron stars.

The parameters of tachyonic self-gravitating body depend on the central density  $\rho_*$  and the tachyon mass  $m$ . For a pure tachyon star its mass and effective radius are plotted in Fig. 2-6, particularly, the maximum mass  $M = 1.18M_\odot$  is achieved at  $m = 939$  MeV. The maximum mass of a tachyonic body at arbitrary  $m$  is determined by universal scaling formula (53) and it is achieved at the same Fermi momentum  $k_F = 1.81m$  (53). While the size of a star with pure neutron content is finite [14], the size of pure tachyon star is unbound. However, we can determine its effective radius (55) under which 99% of the total mass is enclosed. The relevant effective redshift (52) is constant and does not depend on  $m$ .

In practice a stable self-gravitating tachyon body can exist only if it is covered with a non-tachyon envelope because the tachyon matter is unstable when its pressure is below the critical value  $P_T > 0$  (4) and hydrostatic equilibrium condition  $P = 0$  must be achieved somewhere beyond the tachyon matter. We have calculated tachyon stars with three sorts of envelopes: pure neutron matter, neutron-rich matter in the non-linear sigma model [10, 11] and absolute stiff matter (7).

When the tachyon core exists at  $\beta_* = k_F/m > \sqrt{3/2}$ , the total stellar mass  $M_*$  and radius  $r_*$  are greater than those of non-tachyon star. At large  $m$  the main contribution to the total stellar mass is due to the non-tachyonic envelope, and the sort of the envelope is very important here. The tachyon core is relatively small when  $m > 500$  MeV because the critical pressure  $P_T$  (35) and critical density  $\rho_T$  (36) are very large and the tachyon matter is absent in the peripheral region, being concentrated in the very center (Fig. 7-9). As the tachyon mass is chosen small, the critical pressure  $P_T$  (33) is also small, and the tachyon core is larger and more massive (Fig. 10-11). At very small  $m < 200$  MeV the critical pressure  $P_T$  is negligible and the tachyon core occupies almost the whole volume of the star, while the envelope is light and thin (Fig. 12).

Although the parameters of the whole star are much different, the parameters of tachyon core do not depend on the properties of the envelope and all profiles of mass-density  $M_T[\beta_*]$  and radius-density  $r_T[\beta_*]$  obey the scaling (59), see (Fig. 13). The redshift at the surface of tachyon core is given by universal dependence (see, Fig. 14) which is independent of  $m$  and attains maximum value  $z_{\max} \simeq 0.3$  at  $\beta_* \simeq 2.59$ . So, it is enough to perform calculation at a given  $m$  with an arbitrary envelope, and all parameters of the tachyon core with arbitrary  $m$  will be immediately determined by scaling (59). Particularly, the maximum mass and maximum radius are calculated by formula

$$M_{T \max} = 0.52 M_\odot \frac{m_p^2}{m^2} \quad r_{T \max} = 4.07 \text{ km} \frac{m_p^2}{m^2} \quad (60)$$

As soon as the tachyon core appears at  $\beta_* = \sqrt{3/2}$ , its mass  $M_T$  and radius  $r_T$  rapidly increase with increasing  $\beta_*$  until the maximum values are reached, after which the mass and radius decrease at a slow rate. For each  $m$  the mass of tachyon core achieves its maximum value  $M_{T \max}$  at certain  $\beta_* \simeq 2.18$  and the radius of tachyon core achieves its maximum value  $r_{T \max}$

at certain  $\beta_* \simeq 1.61$  (which are the same at any  $m$ ). The density  $\rho_{* \max}$  corresponding to  $\beta_* \simeq 2.18$ , according to (24) and (36), is estimated so

$$\frac{\rho_{* \max}}{\rho_0} \simeq 113\bar{m}^4 \simeq 5.8\rho_T \quad (61)$$

According to formula (60), we find that

$$M_{T \max} \simeq 2000M_\odot \quad r_{T \max} \simeq 18,000 \text{ km} \quad (62)$$

when the tachyon mass is  $m = 14 \text{ MeV}$  and the tachyon critical density is  $\rho_T = 5 \times 10^{-7} \rho_0 = 1.6 \times 10^8 \text{ g} \cdot \text{cm}^{-3}$ , while

$$M_{T \max} \simeq 4 \times 10^{22} M_\odot \quad r_{T \max} \simeq 4 \times 10^{22} \text{ km} \quad (63)$$

when the tachyon mass is  $m = 10^{-11} m_p = 0.01 \text{ eV} \sim 100^\circ K$  and the tachyon critical density is  $\rho_T = 3 \times 10^{-30} \text{ g} \cdot \text{cm}^{-3}$ . The latter value is not so far from the well known observation data about the Universe, and the results of the present paper may find further application to cosmology. The most important property of tachyonic self-gravitating body is that it can exist being embedded in some non-tachyonic medium (whose parameters do not influence the mass and radius of the tachyon core) and that its maximum mass and radius are estimated according to formula (60).

The author is grateful to Erwin Schmidt for discussions.

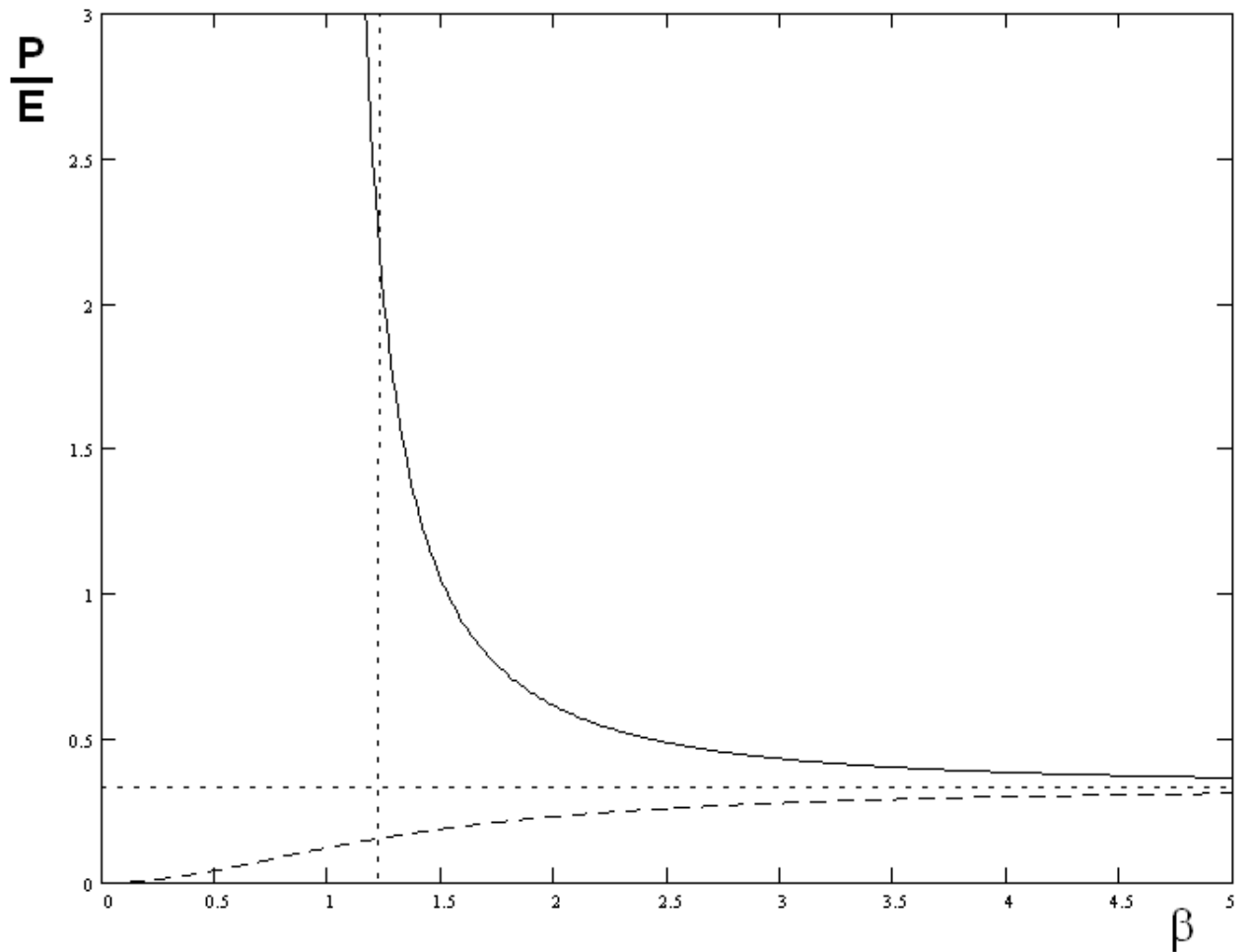
## References

- [1] A. Sen, JHEP **0207**, 065 (2002). [arXiv:hep-th/0203265](#)
- [2] M. C. Bento, O. Bertolami, and A. A. Sen, Phys. Rev. D **67**, 063511 (2003). [arXiv:hep-th/0208124](#)
- [3] A. Frolov, L. Kofman, and A. Starobinsky, Phys.Lett. B **545**, 8 (2002). [arXiv:hep-th/0204187](#)
- [4] E. J. Copeland, M. R. Garousi, M. Sami, S. Tsujikawa, Phys. Rev. D **71**, 043003 (2005). [arXiv:hep-th/0411192](#)
- [5] U. Debnath, Class. Quant. Grav. **25**, 205019 (2008). [arXiv:0808.2379v1 \[gr-qc\]](#)

- [6] St. Mrówczyński, *Nuovo Cim. B* **81**, 179 (1984).
- [7] R. L. Dawe, K. C. Hines and S. J. Robinson, *Nuovo Cim. A* **101**, 163 (1989).
- [8] K. Kowalski, J. Rembielinski, and K.A. Smolinski, *Phys. Rev. D* **76**, 045018 (2007). [arXiv:0712.2725v2](#) [[hep-th](#)]
- [9] E. Trojan and G. V. Vlasov, *Phys. Rev. D* **83**, 124013 (2011). [arXiv:1103.2276](#) [[hep-ph](#)]
- [10] E. Trojan and G.V. Vlasov, *Phys. Rev. C* **81**, 048801 (2010).
- [11] G.V. Vlasov, *Phys. Rev. C* **58**, 2581 (1998).
- [12] J. D. Walecka, *Theoretical nuclear and subnuclear physics*, 2nd. ed. (World Scientific, 2004), p. 19.
- [13] E. Trojan, *Careful calculation of thermodynamical functions of tachyon gas*. [arXiv:1109.10261](#) [[astro-ph.CO](#)]
- [14] J. R. Oppenheimer and G. M. Volkoff, *Phys. Rev.* **55**, 374 (1939).
- [15] C. E. Rhoades and R. Ruffin, *Phys. Rev. Lett.* **32**, 324 (1974).
- [16] V. Kalogera and G. Baym, *ApJ* **470** L61 (1996). [arXiv:astro-ph/9608059](#)
- [17] G.Baym, C. Pethick, and P. Sutherland, *ApJ*, **170**, 299 (1971).

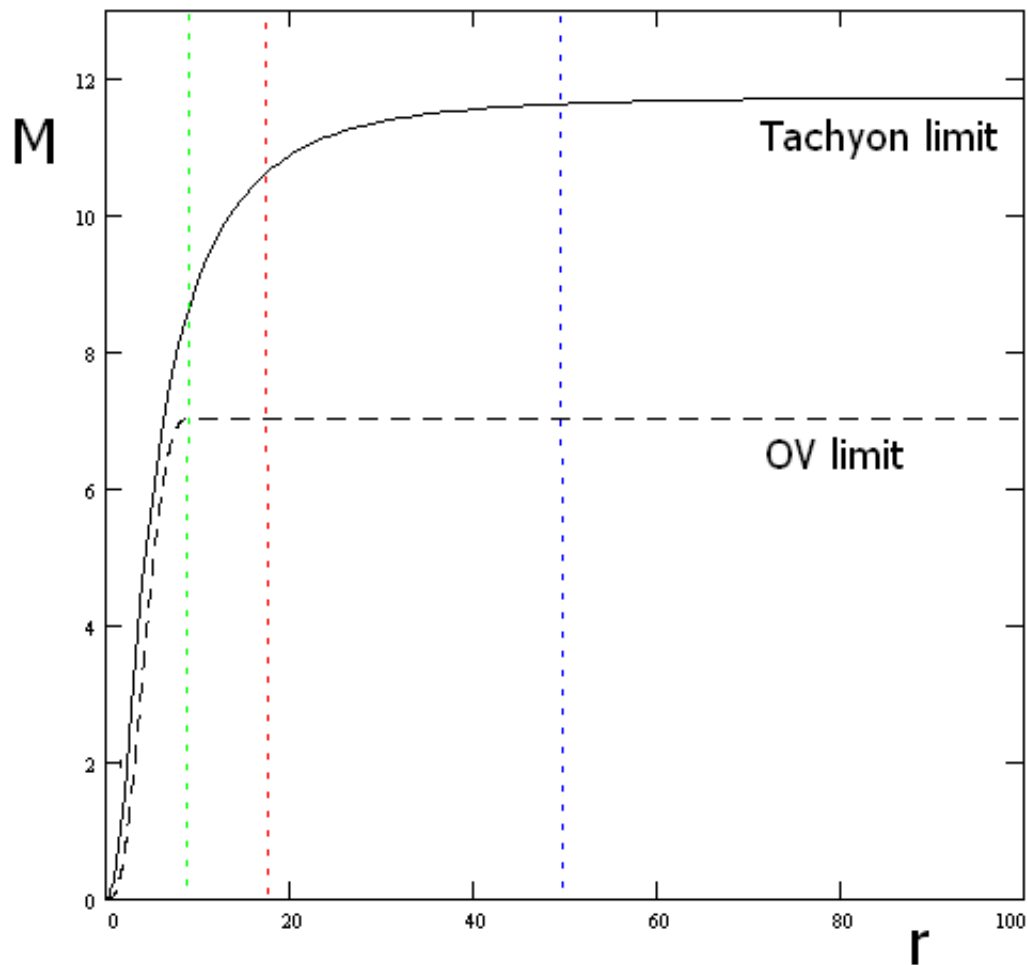


Figure 1: Ratio pressure/energy vs Fermi momentum  $\beta = k_F/m$  for cold Fermi gases of tachyons (solid) and bradyons (dashed).



The tachyon gas is unstable in the left of vertical dotted line (corresponds to  $\beta < \sqrt{3/2}$ ). Horizontal dotted line corresponds to ultrarelativistic gas with  $P/E = 1/3$ .

Figure 2: Mass distribution  $M(r)$  inside a self-gravitating body of pure tachyon matter (solid graph) and pure neutron matter at the same  $m = 939 \text{ MeV}$  (dashed).



The neutron star has finite mass (Oppenheimer-Volkoff limit) and finite radius (green vertical line), the tachyon star has finite mass and infinite radius. Blue vertical line cuts 90%, red vertical line cuts 99% of the total mass of tachyon star.

Figure 3: Mass of tachyonic self-gravitating body vs central density.

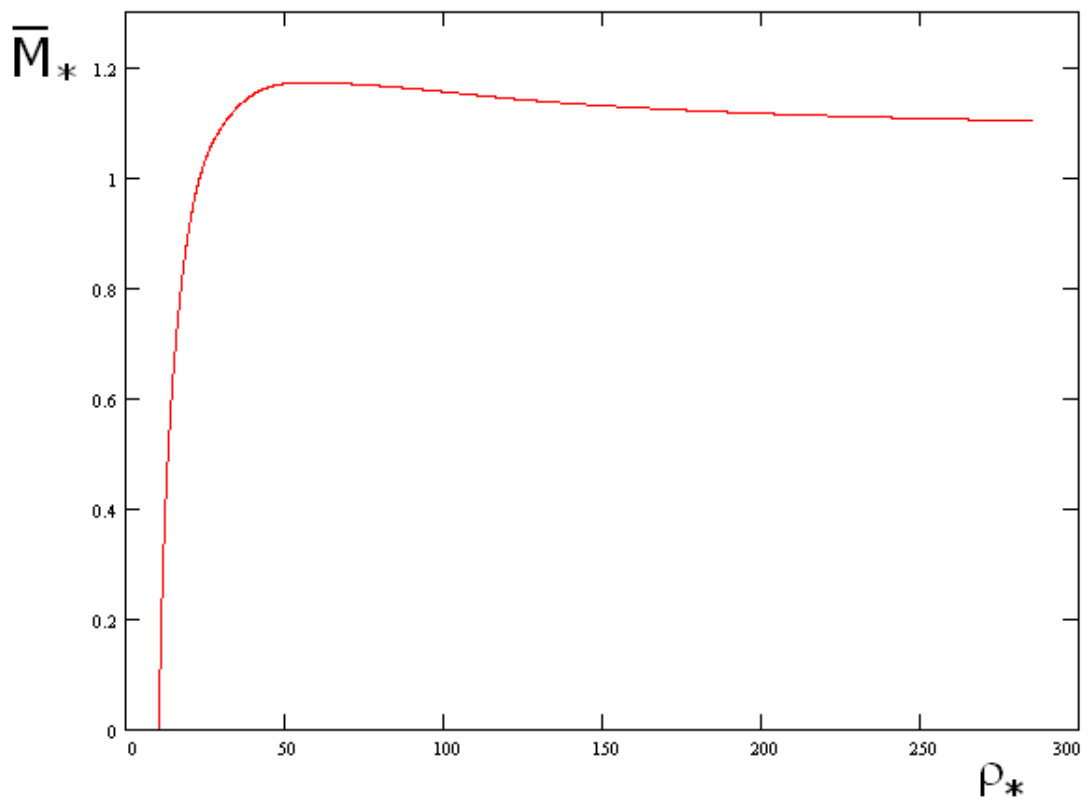
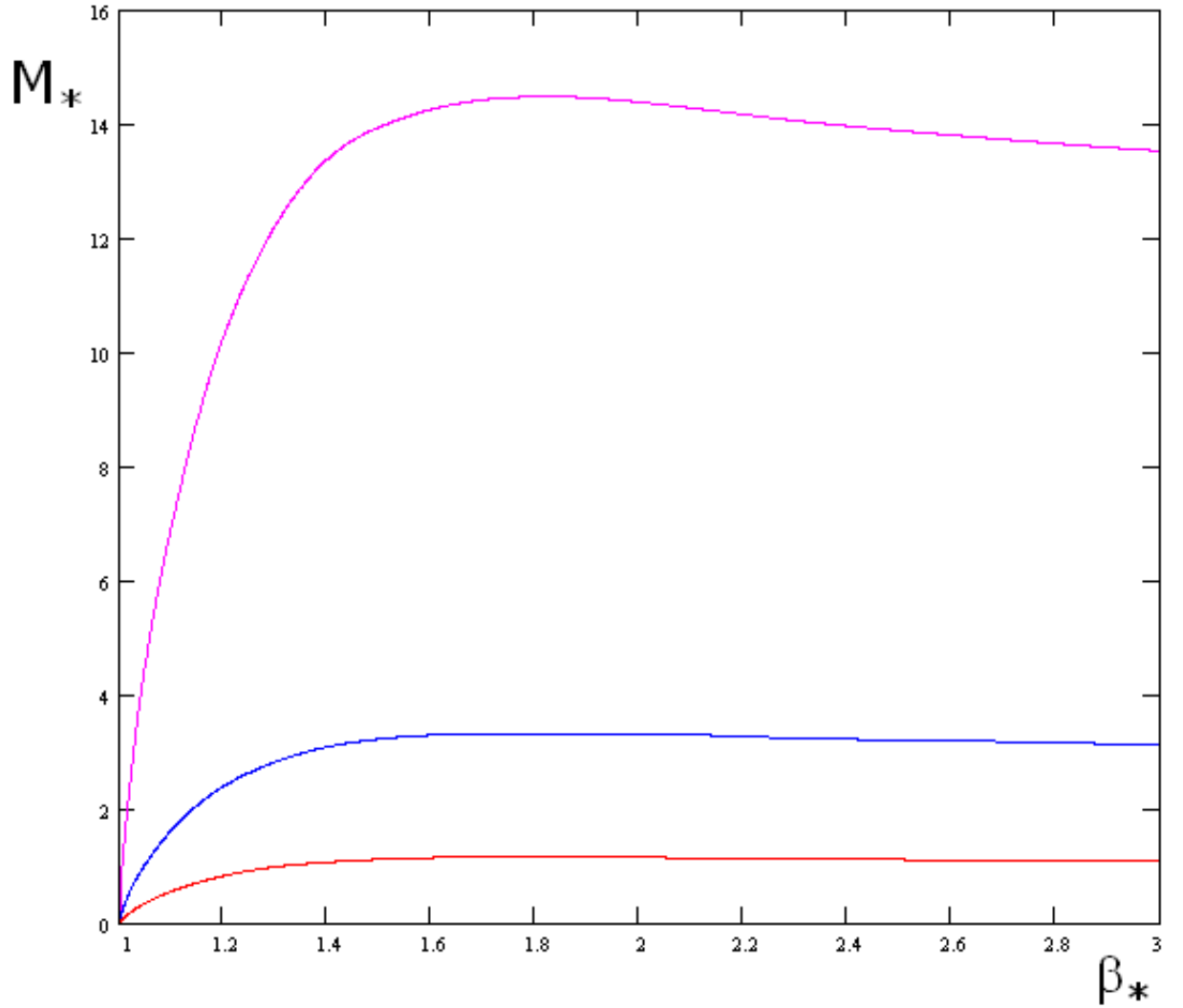


Figure 4: Mass of tachyonic self-gravitating body vs variable.



At  $m = 266$  MeV (pink),  $m = 666$  MeV (blue) and  $m = 939$  MeV (red).

Figure 5: Effective radius  $\bar{r}_{99}$  (red) and  $\bar{r}_{90}$  (blue) of tachyonic self-gravitating body vs central variable  $\beta_*$ .

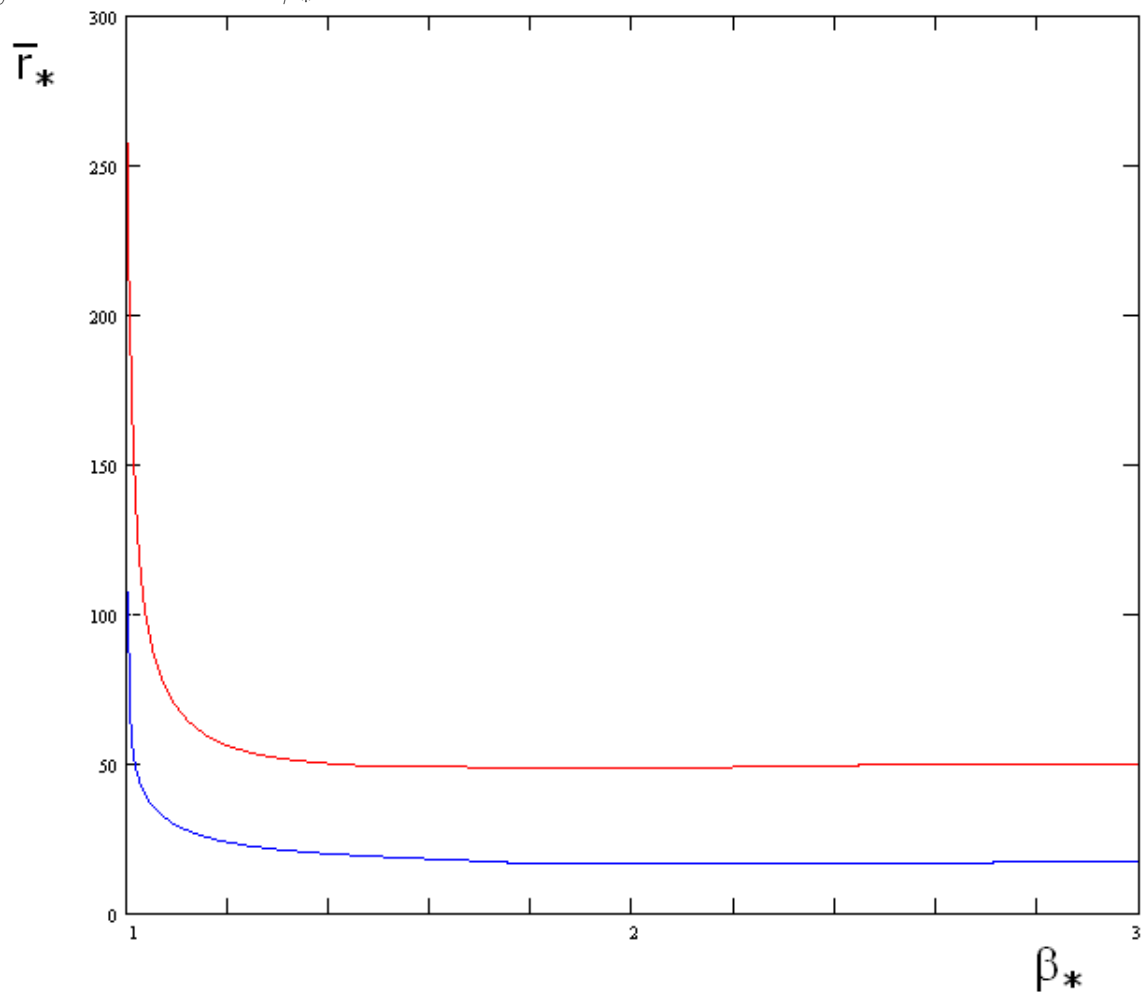


Figure 6: The profile of redshift  $z(r)$  inside the tachyonic body at different central density:  $\beta_* = 1.5$  (solid line),  $\beta_* = 2.5$  (dashed),  $\beta_* = 5$  (dotted) and maximum redshift  $z_{\max}$  vs  $\beta_*$ .

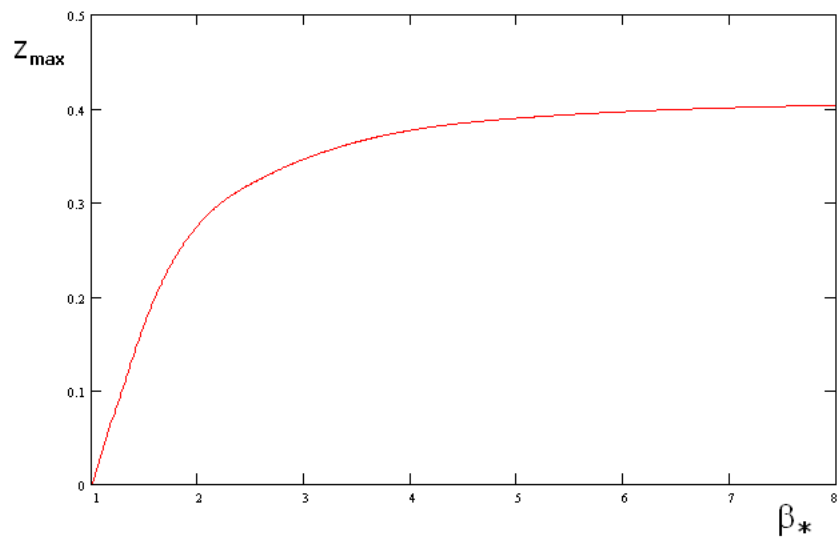
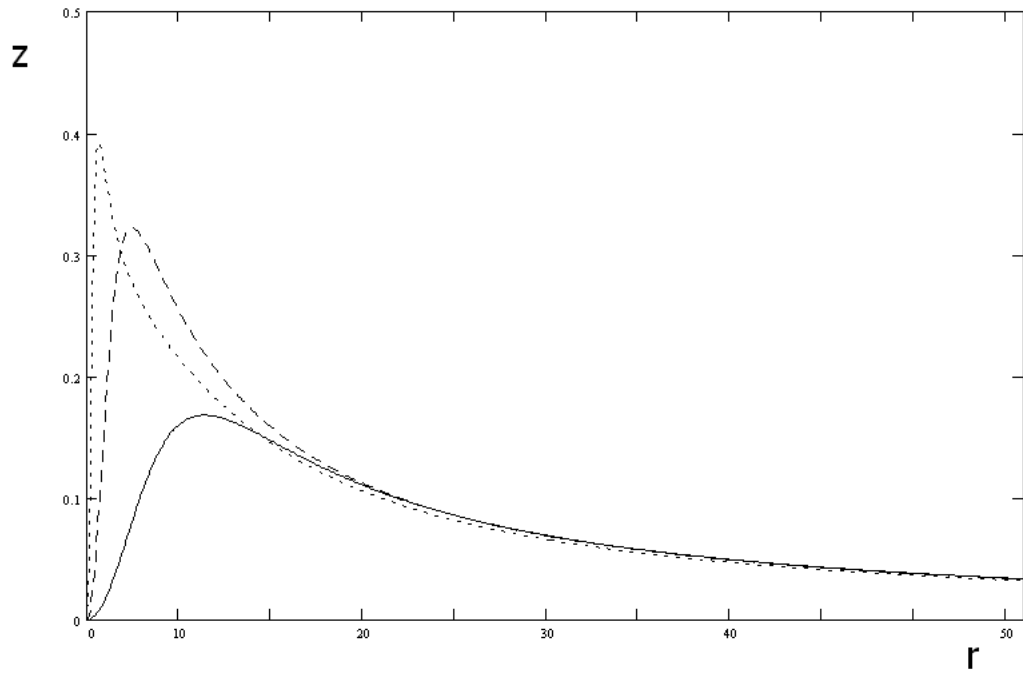
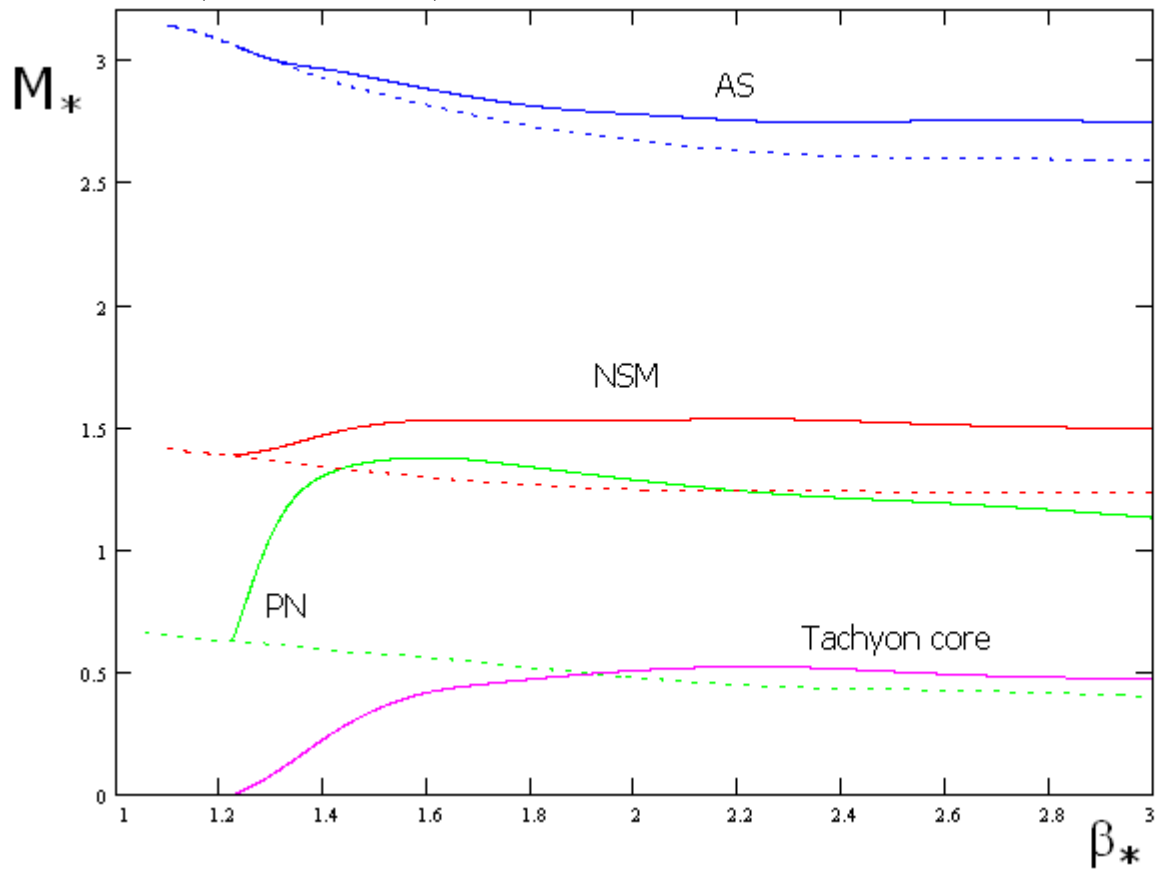
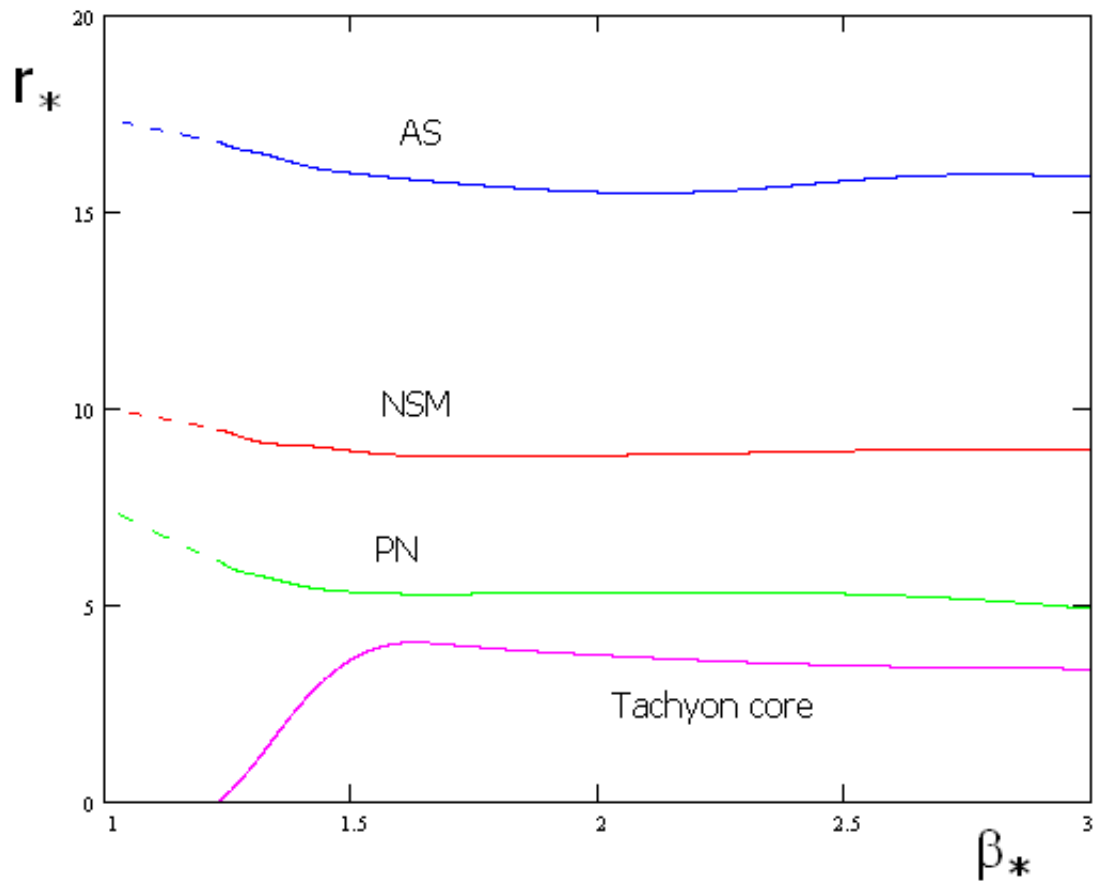


Figure 7: The mass of a star with tachyon core and three types of envelope vs variable  $\beta_*$  (at  $m = 939$  MeV).



Dashed line corresponds to a star with no tachyon content.

Figure 8: The radius of a star with tachyon core and three types of envelope vs  $\beta_*$  ( $m = 939 \text{ MeV}$ ).



Notation is the same as in Fig. 7. The radius of tachyon core is given in PINK.



Figure 9: The mass and radius of a star with tachyon core in PN envelope vs variable  $\beta_*$  (at  $m = 666$  MeV).

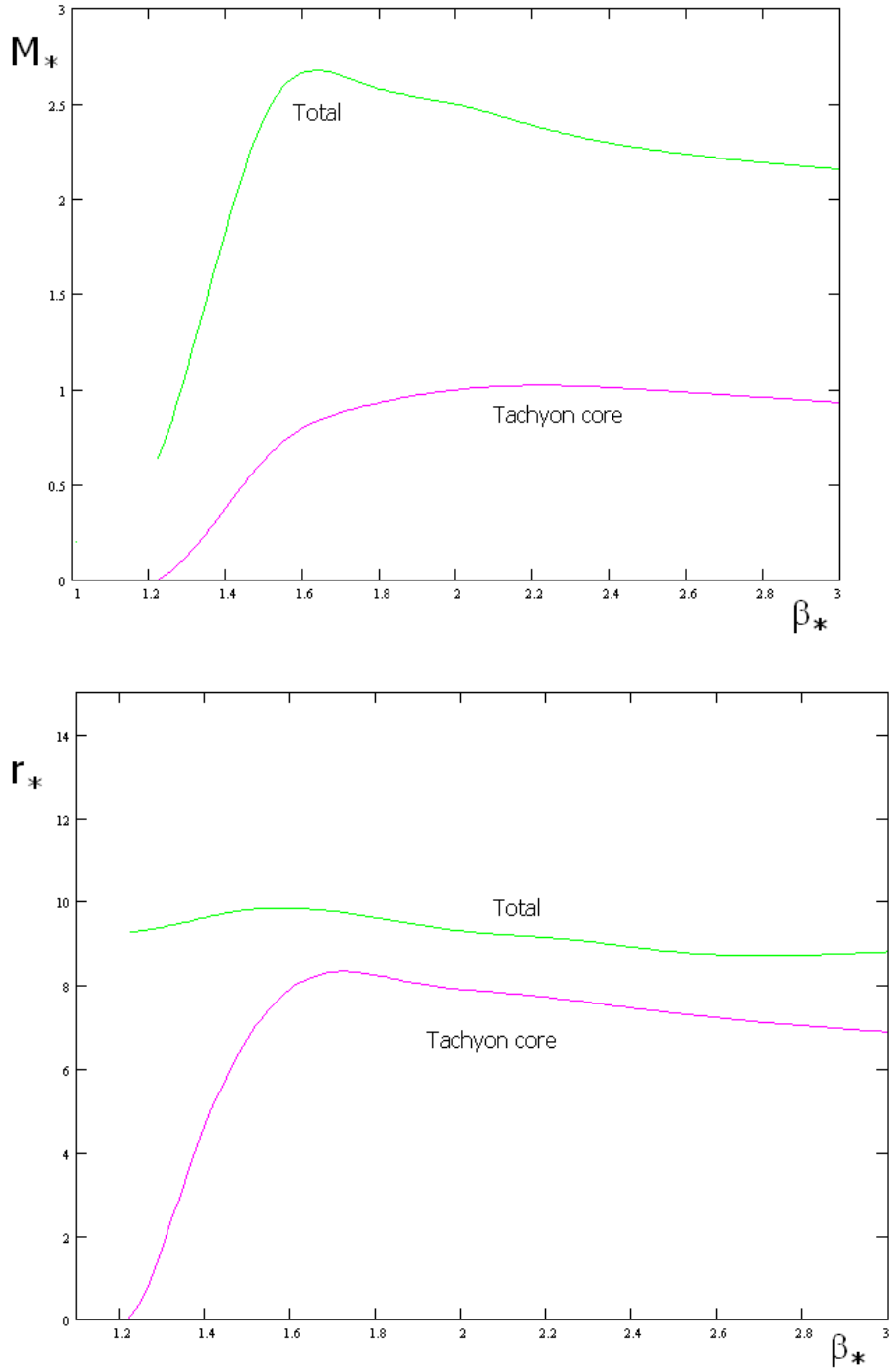


Figure 10: The mass and radius of a star with tachyon core in PN envelope vs variable  $\beta_*$  (at  $m = 400$  MeV).

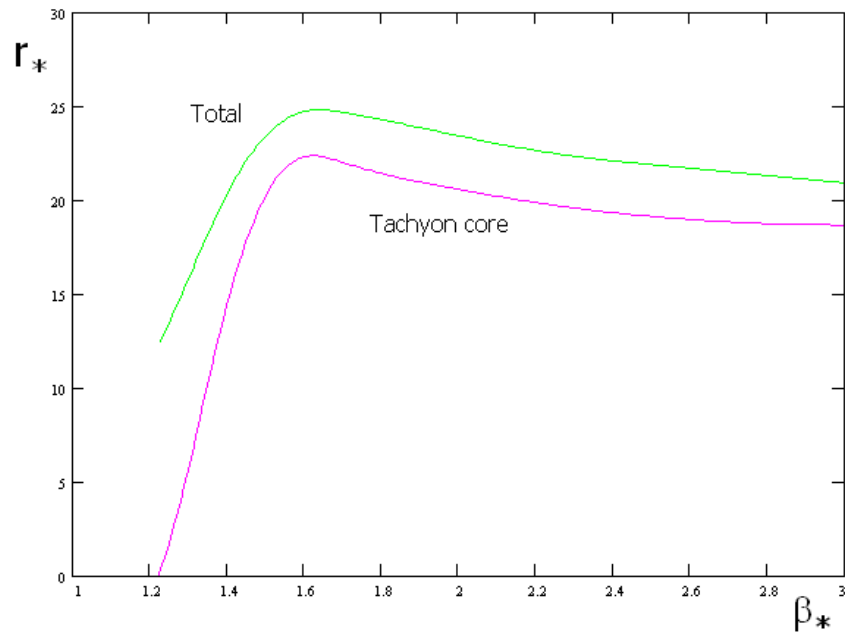
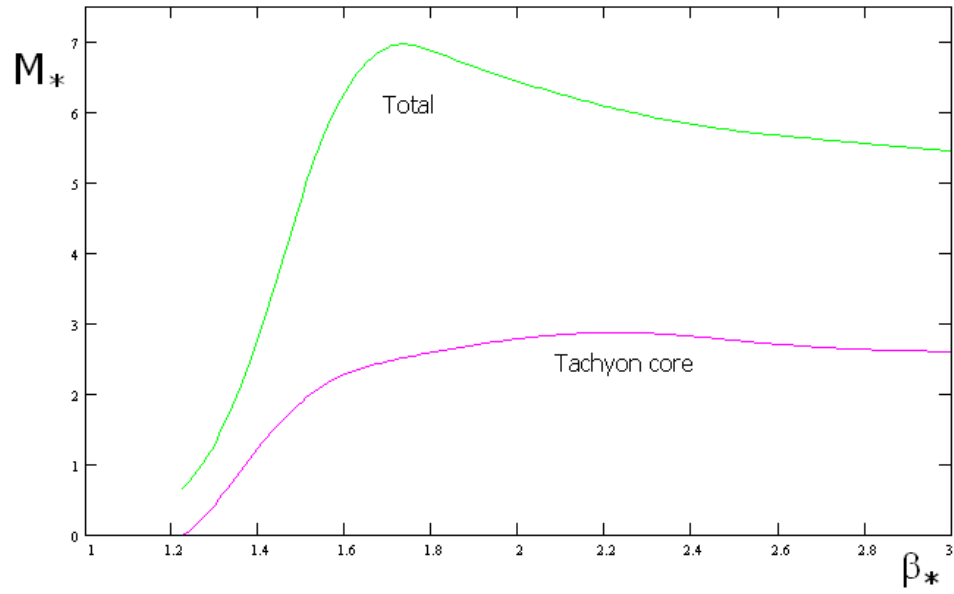


Figure 11: The mass and radius of a star with tachyon core in PN envelope vs variable  $\beta_*$  (at  $m = 233$  MeV).

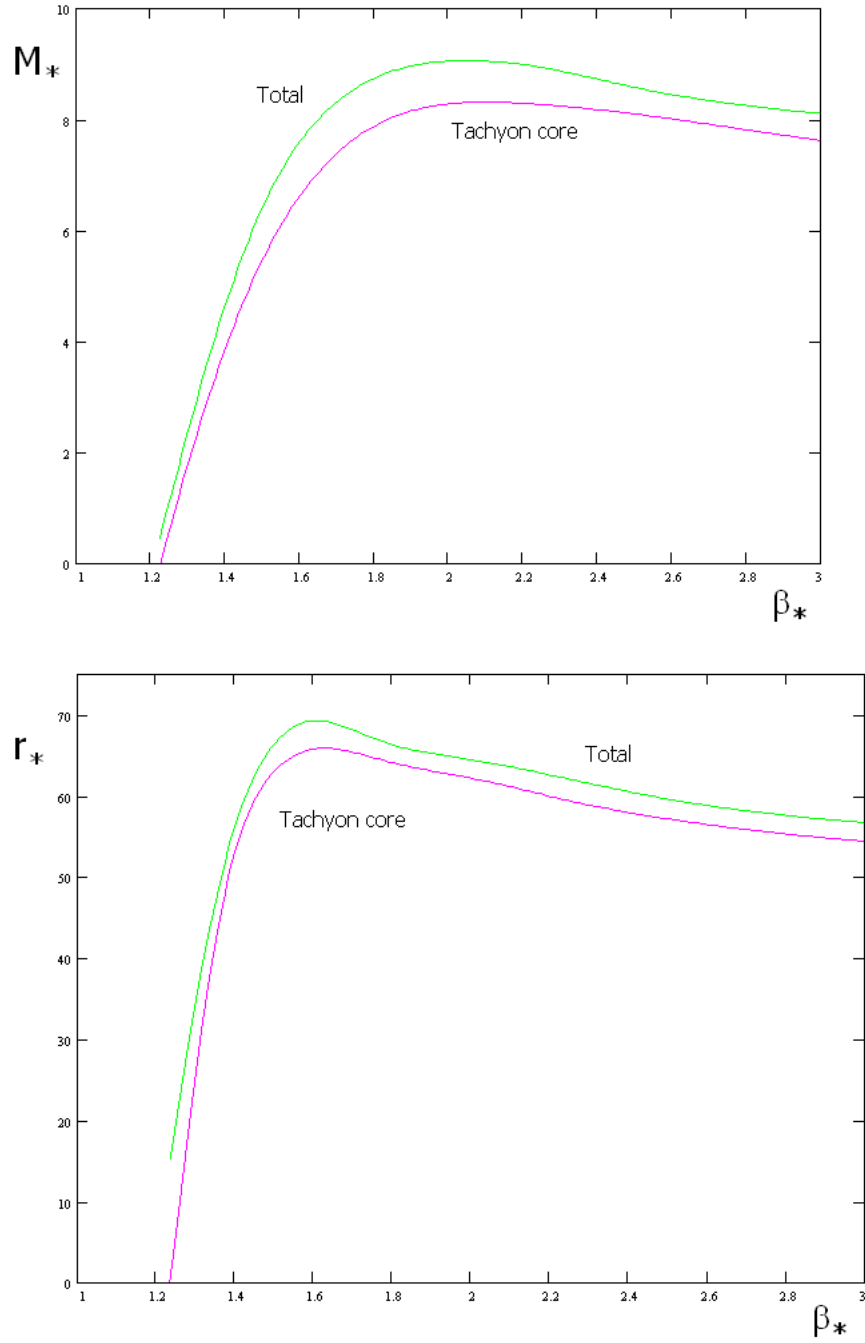


Figure 12: The mass and radius of a star with tachyon core in PN envelope vs variable  $\beta_*$  (at  $m = 138$  MeV).

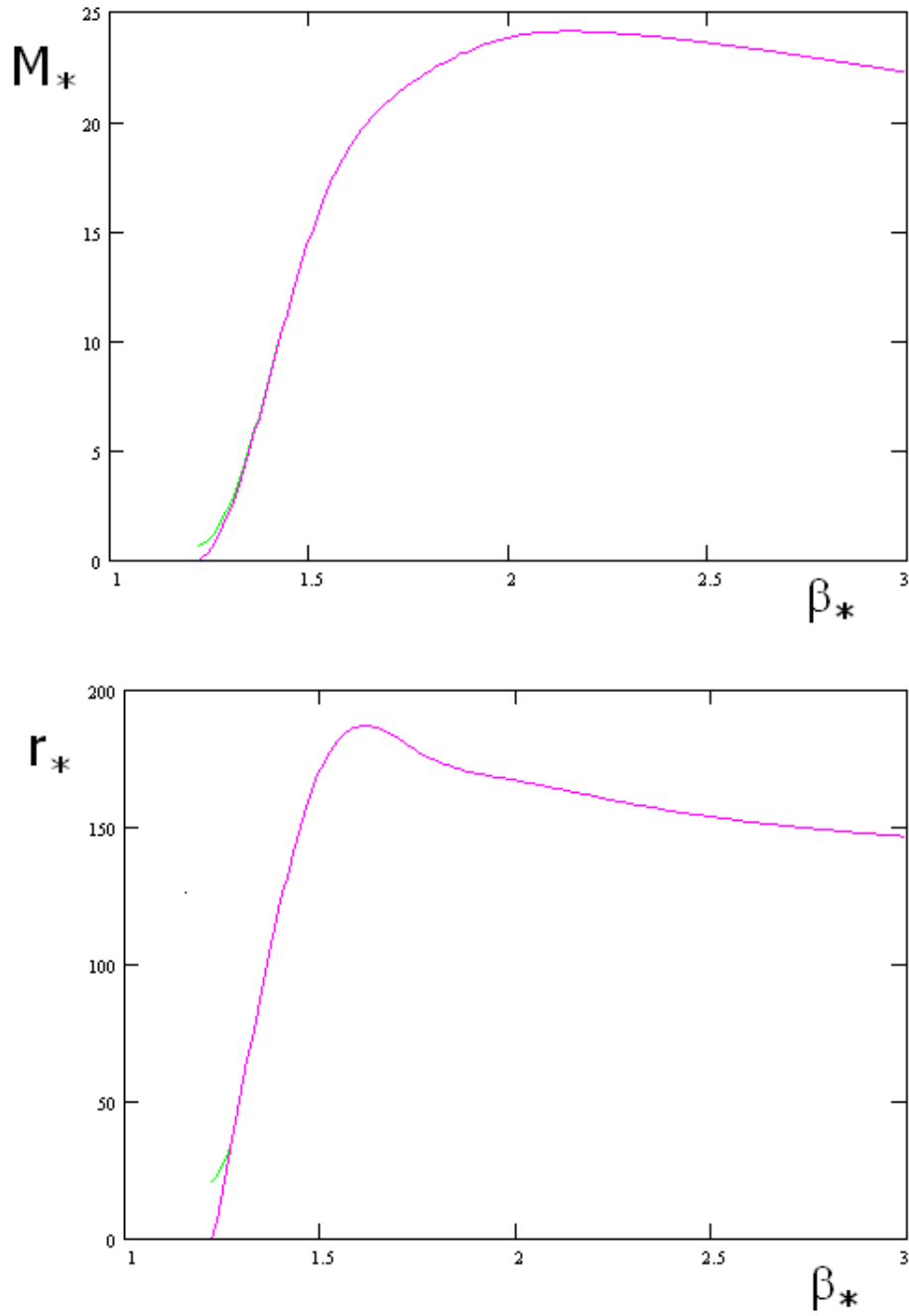


Figure 13: The mass and radius of tachyon core  $\bar{M}_T[\beta_*]$  at  $m = 939$  MeV.

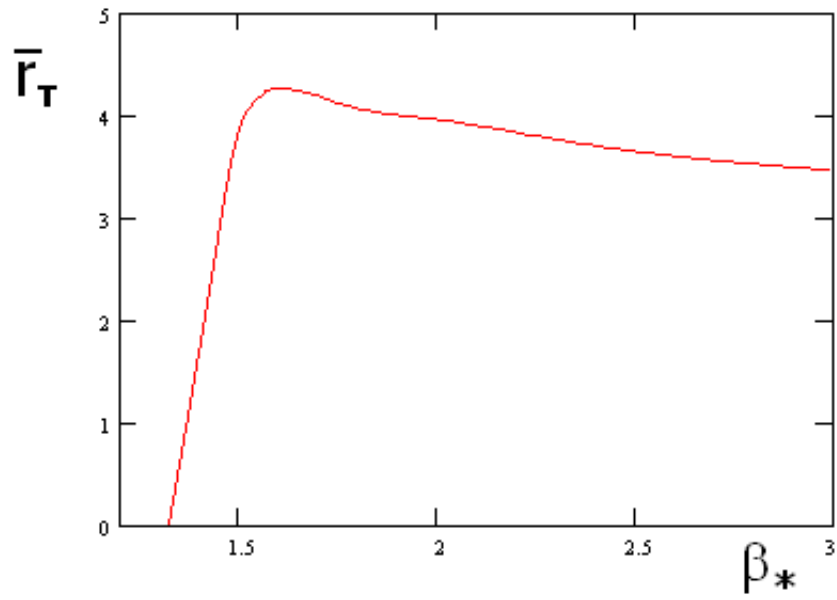
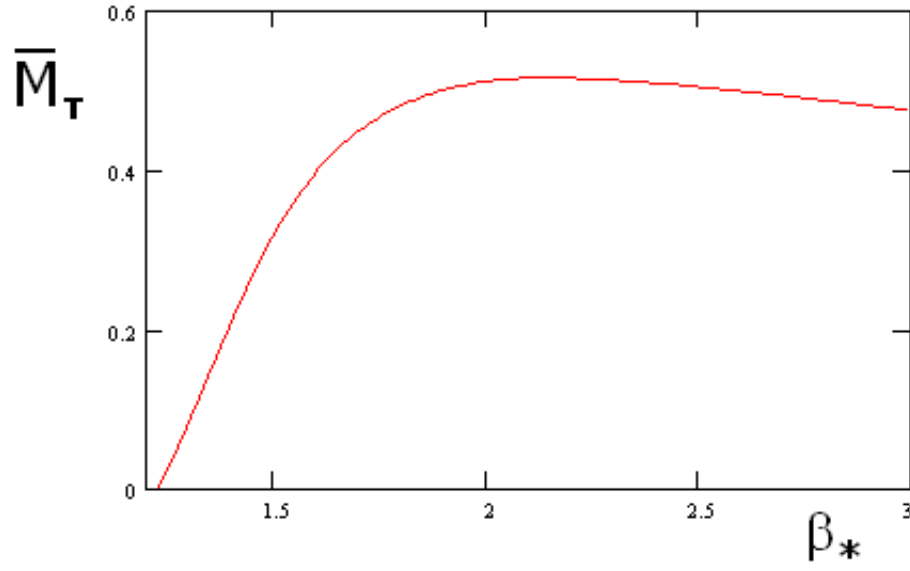


Figure 14: The redshift at the surface of the tachyon core vs  $\beta_*$ .

